Adaptive Sampling and Processing of Ultrasound Images

Paul Rodríguez V. and Marios S. Pattichis

image and video Processing and Communication Laboratory (ivPCL)
Department of Electrical and Computer Engineering, The University of New Mexico,
Albuquerque, NM, 87131
e-mail: {prodrig,pattichis}@eece.unm.edu

Abstract -*An AM-FM video image representation is developed and applied to M-mode ultrasound. The AM-FM representation describes the video in terms of an AM-FM series expansion. For estimation, the fundamental AM-FM harmonic is estimated using a collection of bandpass filters that are adaptively selected so that one with the maximum response is selected. For each bandpass filter, the output image is downsampled depending on the spectral support of the filter. Using results from multidimensional Frequency Modulation theory, it is shown that a fast separable implementation is possible. In turn, good estimates are obtained from a collection of only two separable, bandpass filters approximated with just a small number of 11 coefficients and the recently developed SIMD-FFT. The fundamental AM-FM harmonic is seen to capture the essential structure of the image and simple thresholding of the amplitude estimate yields very good segmentation results.*

1. Introduction

Cardiac ultrasound video is highly non-stationary. In M-mode ultrasound video, a ray of points is tracked through time, leading to an observation of cardiac wall motion moving through time (M in M-mode stands for motion).

To recognize a suitable AM-FM series for the M-mode image ultrasound image, consider the idealized curvilinear coordinate system $\psi - \phi$ where ψ traces the equi-intensity contours of the moving walls, while ϕ moves in the direction of the gradient of the intensity image (see Figure 2(c)). Then, the Fourier-series along the curvilinear coordinates is an AM-FM-series in the original space-time coordinates $x - t$ (also see [2]):

$$f(x,t) = \sum_n C_n \cos(n\phi(x,t)) \quad (1)$$

To generalize our example in order to account for slowly-varying object brightness variation, we also introduce a spatially-varying amplitude, and modify the fundamental equation to (where the time coordinate t coincides with the y coordinate in M-mode ultrasound):

$$f(x,y) = \sum_n C_n\, a(x,y)\cos(n\phi(x,y)) \quad (2)$$

The AM-FM series expansion proposed by (2) will be used for modeling the ultrasound video. The AM-FM demodulation problem estimates the amplitude $a(x,y)$, the phase $\phi(x,y)$, and the instantaneous-frequency vector $\nabla\phi(x,y) = [\partial\phi/\partial x, \partial\phi/\partial y]^T$.

To estimate the AM-FM parameters, we usually apply a collection of Gabor (bandpass) channel filters $g_1, g_2, ..., g_R$ to the image f, obtaining output images $h_1, h_2, ..., h_R$ satisfying $h_i = f * g_i$ where * denotes convolution. Let $G_1, G_2, ..., G_R$ denote the frequency responses of the Gabor channel filters. We then obtain estimates for the instantaneous frequency and the phase using [2-4]:

$$\nabla\phi_i(x,y) \cong \text{real}\left\{\frac{\nabla h_i(x,y)}{j h_i(x,y)}\right\},$$

$$\phi_i(x,y) \cong \arctan\left\{\frac{\text{imaginary}\{h_i(x,y)\}}{\text{real}\{h_i(x,y)\}}\right\}. \quad (3)$$

Using the instantaneous frequency estimate $\nabla\phi(x,y)$ and the frequency response of the Gabor channel G_i, we estimate the amplitude over each channel using

0-7803-7147-X/01/$10.00©2001 IEEE

$$a_i(x,y) \cong \left| \frac{h_i(x,y)}{G_i(\nabla\phi(x,y))} \right|. \quad (4)$$

In the Dominant Component Analysis (DCA) algorithm, from the estimates for each channel filter, we select the estimates from the channel with the maximum amplitude estimate: $c_{\max}(x,y) = \underset{i}{\operatorname{argmax}}\ a_i(x,y)$. Hence, the algorithm adaptively selects the channel filter with the maximum response. This approach does not assume spatial continuity, and allows the model to quickly adapt to singularities in the image. The performance of the AM-FM demodulation algorithm in one and two-dimensions has been studied in [2-4]. A discrete-space algorithm is also described in [2,3].

In Section 2, we summarize the main concepts of multidimensional Frequency modulation as they were originally developed in [2]. In Section 3, an efficient, separable 1-D implementation is described. The results are summarized in Section 4, and some concluding remarks are made in Section 5.

2. Multidimensional Frequency Modulation

To understand multidimensional frequency modulation, we evaluate the component derivatives of the instantaneous frequency vector $[\partial\phi/\partial x,\ \partial\phi/\partial y]^T$ to compute [2,5]:

$$\mathbf{F}(\mathbf{p}) = \begin{bmatrix} \partial^2\phi(\mathbf{p})/\partial x^2 & \partial^2\phi(\mathbf{p})/\partial y\partial x \\ \partial^2\phi(\mathbf{p})/\partial x\partial y & \partial^2\phi(\mathbf{p})/\partial y^2 \end{bmatrix} \quad (5)$$

where $\mathbf{F}$ denotes the Instantaneous Frequency Gradient Tensor (IFGT). The IFGT is real symmetric and hence allows an eigen-decomposition:

$$\mathbf{F}(\mathbf{p}) = \begin{bmatrix} \uparrow & \uparrow \\ \mathbf{e}_1 & \mathbf{e}_2 \\ \downarrow & \downarrow \end{bmatrix} \begin{bmatrix} \lambda_1 & \\ & \lambda_2 \end{bmatrix} \begin{bmatrix} \leftarrow & \mathbf{e}_1 & \rightarrow \\ \leftarrow & \mathbf{e}_2 & \rightarrow \end{bmatrix}. \quad (6)$$

The eigen-decomposition can then be used to establish the dominant Frequency Modulation bounds [2]:

$$|\lambda_1|\|d\mathbf{p}\| \le \|d\mathbf{O}\| \le |\lambda_2|\|d\mathbf{p}\|, \quad |\lambda_1| \le |\lambda_2| \quad (7)$$

where $d\mathbf{P} = [dx, dy]^T$, the minimum is attained along the direction of the first eigenvector, while the maximum is attained along the second eigenvector.

The FM equations summarized in (5-7) can be used to develop an intuitive, geometrical understanding of multidimensional Frequency Modulation. We note that the FM parameters describe a local, quadratic approximation to the phase. Hence, to interpret the FM parameters, we examine the non-stationary image structure locally. For example, for positive eigenvalues, the local image structure approximates simple, concentric, ellipsoidal deformations, where the dominant eigenvector is associated with the major axis where the instantaneous frequency magnitude is changing most rapidly. Orthogonal to that direction is the eigenvector associated with the smallest eigenvalue. The eigenvector is associated with the smallest eigenvalue points in the direction of the minor ellipsoidal axis, where the instantaneous frequency vector magnitude undergoes minimal increase.

Along the eigenvector direction, the phase is approximately separable [2]:

$$\exp[j\phi(z_1, z_2)] \approx \exp[j\phi_1(z_1)]\exp[j\phi_2(z_2)] \quad (8)$$

where the $z_1 - z_2$ coordinates are the image trajectories of the eigenvectors. The approximation is met with equality if the approximations: $d\mathbf{z}/ds \approx \mathbf{E}\, d\mathbf{p}/ds$, $d\mathbf{z}/ds^2 \approx \mathbf{E}\, d^2\mathbf{p}/ds^2$ hold exactly (where $\mathbf{E}$ denotes the spatially-varying eigenvector matrix). It can be shown that the approximation error can be bounded provided that the eigenvectors do not rotate along the trajectory [2].

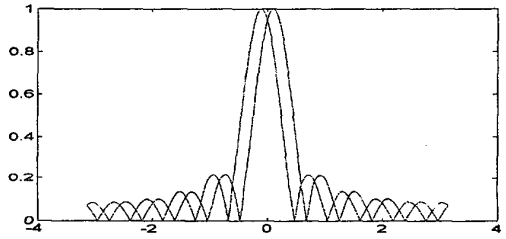

(a)

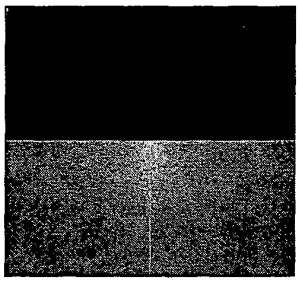

(b)

Figure 1. Separable 1-D filter design. In 1(a), the magnitude response of the two 1-D filters is shown. In 1(b), the spectrum of the "analytic image" is shown. For the 1-D designs, only 11 filter coefficients are used.

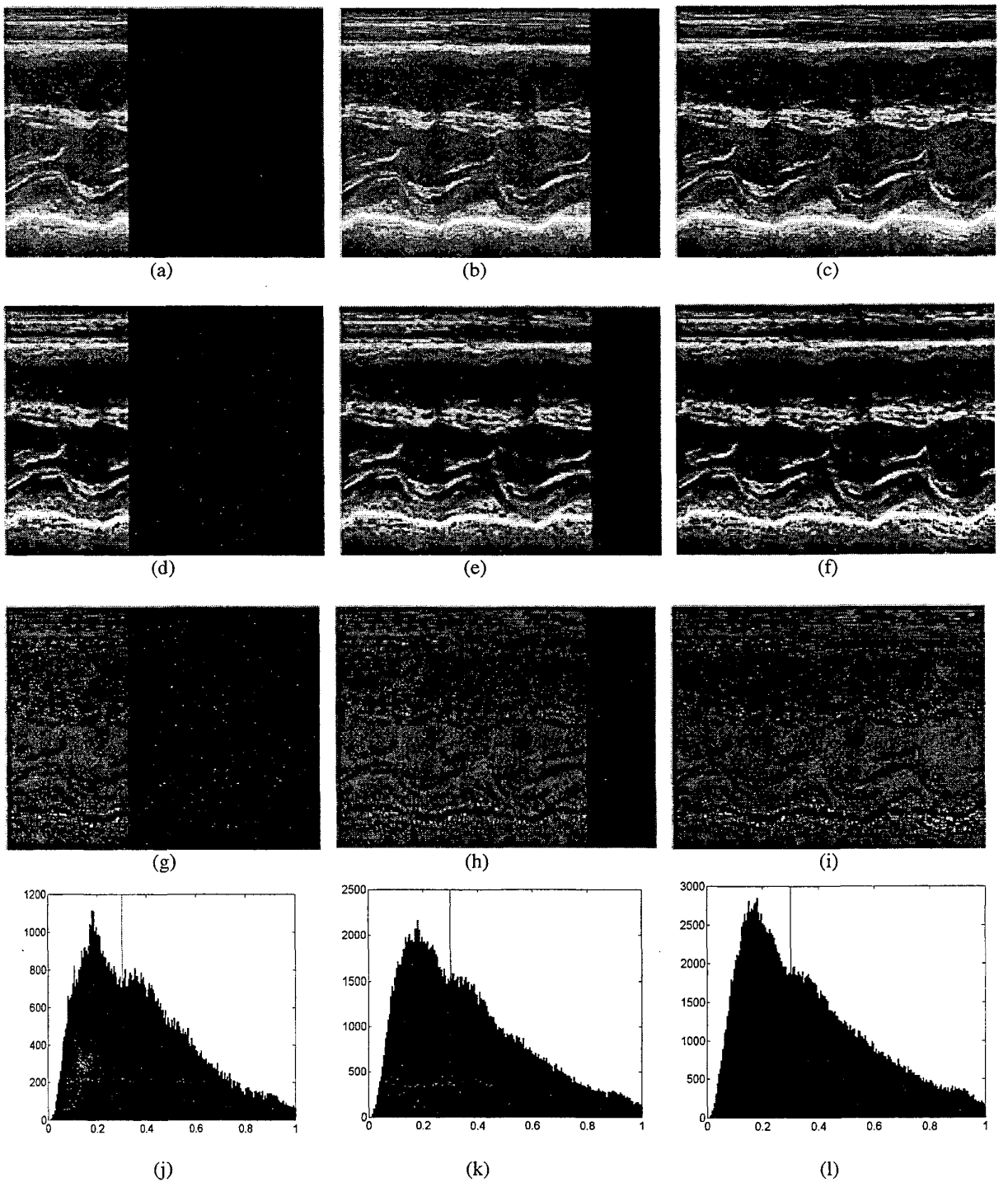

Figure 2. AM-FM Segmentation Results. The original video images are shown in figure 2(a)-(c). The segmented image is selected by picking a threshold that is close to separating two somewhat independent distributions (2(j)-2(l)). In 2(d)-(f), the portion of the image with amplitude more that 0.3 is shown, while in 2(g)-(i), the portions of the images with amplitude less than 0.3 is shown. In 2(j)-(l) the histogram of the AM demodulated image is shown for all cases.

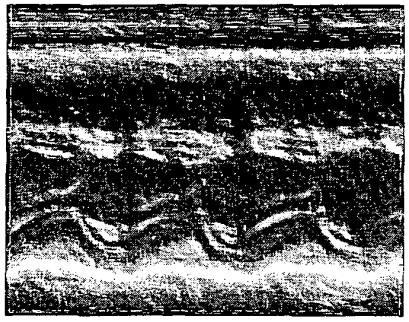

(a) AM reconstruction

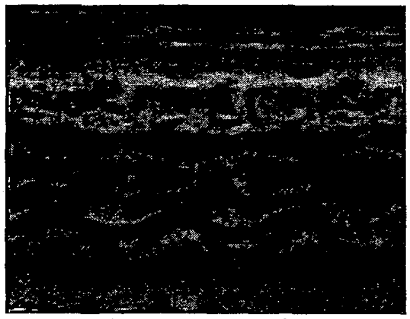

(b) FM reconstruction

(c) AM-FM reconstruction

Figure 3. AM-FM Reconstructions using only the fundamental harmonic only. In 3(a), the reconstructed amplitude $a(x, y)$ is shown, in 3(b), the reconstructed FM function $\cos\phi(x, y)$ is shown, while in 3(c), the reconstructed AM-FM function $a(x, y)\cos\phi(x, y)$ is shown.

3. Fast AM-FM Demodulation

For performing AM-FM demodulation, a separable 1-D filter design method was used. The 1-D profiles for the 1-D filters are shown in Figure 1(a). Each filter is approximated by only 11 coefficients. Prior to bandpass filtering, the original image was used to generate its "analytic" extension as shown in Figure 1(b). For computing the analytic extension, a fast FFT algorithm was used that is described in [6].

At each pixel, the filter that produced the highest amplitude estimate was used. This allowed for the demodulation system to adaptively adjust to the spatial variations of the image. The Quasi-Eigenfunction Approximation (QEA) was used for correcting the outputs from each filter.

Figure 4. AM-FM reconstruction using spatially-selective filtering. At each pixel in the image, the bandpass filter with the maximum amplitude response is selected. The output of each filter is downsampled by 3×3, three times along the vertical and three times along the horizontal directions. The image was reconstructed after upsampling in the same way, and using the same bandpass filters.

4. Results

The results are summarized in Figure 2 for AM-FM image segmentation, Figures 3 and 4 for image reconstruction, and AM-FM image parameters in Figure 5.

In the AM-FM segmentation results in Figure 2, M-mode images are shown in 2(a)-2(c), the corresponding foreground pixels, including the valve and the cardiac walls, are shown in Figures 2(d)-2(f), while the backscatter pixels are shown in Figures 2(g)-2(i). The histogram of the estimated amplitude is shown in Figures 2(j)-2(l). The segmentation algorithm simply selected low amplitude pixels as backscatter pixels while high amplitude pixels capture the valve and the cardiac walls.

In Figures 3 and 4, the results of image reconstruction from the estimated AM-FM parameters are shown. In Figure 5, it is clear that the estimated eigenvectors of the instantaneous frequency gradient tensor are aligned along the horizontal and vertical coordinates.

This implies that the most significant frequency modulation in the image actually occurs along the horizontal and vertical directions. This observation supports the argument that the phase estimate can be considered to be separable along the horizontal and vertical coordinates. In turn, this is evidence in support of the separable processing design of Figure 1. Thus, for the AM-FM reconstruction in Figure 4, the image was downsampled along the horizontal and vertical coordinates, by a factor of three in each coordinate. For both Figures 3 and 4, only the fundamental AM-FM harmonic is used for the reconstruction.

5. Conclusion and Ongoing Work

The proposed AM-FM representation for M-Mode ultrasound video has proven very effective in both describing the rapid deformations as well as efficiently representing the essential structure of the ultrasound images. Fast AM-FM demodulations are possible using one-dimensional designs, and fast, yet very effective, segmentation was demonstrated using simple thresholding of the estimated amplitude.

Currently, the image and video Processing and Communication Lab (ivPCL) is developing a 3-D ultrasound video system for reconstructing 3-D models of the heart from freehand, B-mode ultrasound. The AM-FM model will be extended into 3-D for processing the acquired video and also representing the cardiac deformations through time.

6. Acknowledgment

The authors would like to thank the Echocardiography Lab in the Children's Heart Center for providing us with the cardiac ultrasound.

References

[1] X. Papademetris and J. S. Duncan, "Cardiac Image Analysis: Motion and Deformation," in *Handbook of Medical Imaging: Processing and Analysis,* edited by M. Sonka and J. M. Fitzpartrick, pp. 675-710, SPIE Press, Bellingham, Washington, 2000.

[2] M.S. Pattichis, "AM-FM Transforms with Applications." Ph.D. diss., The University of Texas at Austin, 1998.

[3] J.P. Havlicek, "AM-FM Image Models." Ph.D. diss., The University of Texas at Austin, 1996.

[4] M. S. Pattichis, G. Panayi, A. C. Bovik, and H. Shun-Pin, "Fingerprint Classification Using an AM-FM Model," *IEEE Transactions on Image Processing,* vol. 10, no. 6, pp. 951-954. June 2001.

[5] M.S. Pattichis and A.C. Bovik, "Multi-Dimensional Frequency Modulation in Texture Images," in *Proc. International Conference on Digital Signal Processing,* Limassol, Cyprus, June 26-28 1995, pp. 753-758.

[6] P. Rodríguez V, "A Radix-2 and FFT Algorithm for Modern Single Instruction Multiple Data (SIMD) Architectures, " submitted to *Signal Processing Letters.*

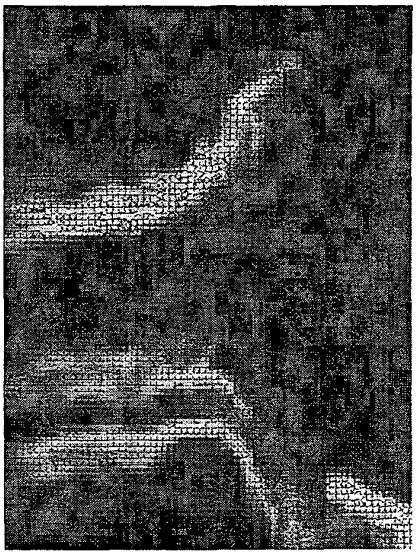

(a) eigenvector estimates.

(b) instantaneous frequency vector estimation

Figure 5. AM-FM parameter estimation over segmented region. The subimage presented here corresponds to the last frame in 2(c). It contains the valve motion over the first cycle (lower left part of the image). Small dots are shown over the non-segmented pixels.